

Ruthenium Carbonyl Complexes Bearing Secondary Phosphine Oxides and Phosphinous Acids: Synthesis, Characterization, and Application in Catalysis

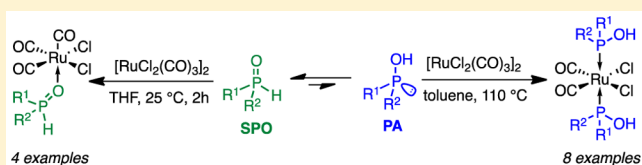
Lionel V. Graux,[†] Michel Giorgi,[‡] Gérard Buono,^{*,†} and Hervé Clavier^{*,†}

[†]Aix Marseille Université, Centrale Marseille, CNRS, iSm2 UMR 7313, 13397, Marseille, France

[‡]Aix Marseille Université, Spectropole, Fédération des Sciences Chimiques de Marseille, 13397 Marseille, France

Supporting Information

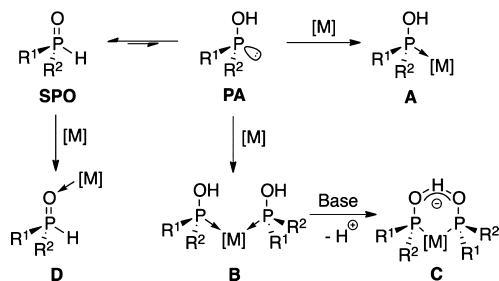
ABSTRACT: Two series of ruthenium carbonyl complexes bearing either one secondary phosphine oxide ligand or two phosphinous acids have been synthesized and characterized. The catalytic behavior of these complexes has been then investigated for the cycloisomerization of arenynes. This study highlighted a strong relationship between ligands' and substrates' substructures.



INTRODUCTION

Secondary phosphine oxides (SPO) and phosphinous acids (PA) are interesting phosphorus compounds, especially as ligands in coordination chemistry.¹ As depicted in Scheme 1, a

Scheme 1. Tautomeric Equilibrium between SPO and PA and Their Resulting Coordination Modes



tautomeric equilibrium between the tricoordinated trivalent ($\sigma^3\lambda^3$) phosphinous acid and the tetracoordinated pentavalent ($\sigma^4\lambda^5$) phosphine oxide form does exist in solution² and is generally completely shifted in favor of the phosphine oxide form. Nevertheless, the P(III) compound can coordinate a transition metal to afford complexes **A** or **B** bearing respectively one or two PA units. In this case, SPOs are considered as preligands. In the presence of base, **B** is converted into complex **C** bearing the phosphinito-phosphinous acid pincer ligand. The study of the electronic properties of these ligands showed comparable electron-donating abilities between phosphinous acids and the corresponding phosphines, but phosphinito ligands are significantly more donating.³ Alternatively, SPO can coordinate the metal through the oxygen atom to give rise to complex **D**. However, this mode of coordination has been scarcely observed, mainly with rare earth metals,⁴ early transition metals,⁵ or group 13 elements.⁶ To the best of our

knowledge, for late transition metals, only a few examples have been reported. With nickel, these complexes are difficult to isolate (32% yield in the best case),⁷ and with rhodium, complexes **D** have been only observed in solution.^{3,8} The intricacy of SPOs' and PAs' coordination modes might explain why these ligands have been little investigated so far.

Yet, they have attracted an ever-growing attention since Li reported that PA-containing palladium complexes are com-

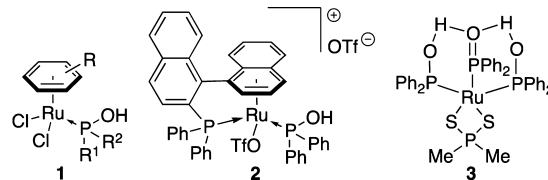
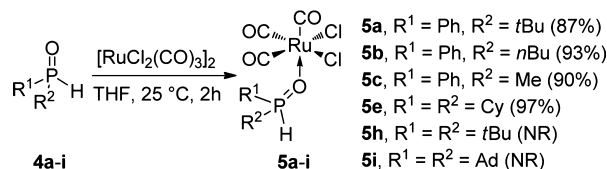


Figure 1. Ruthenium complexes bearing PA or SPO ligands.

petent to perform C–C and C–X bond formations by cross-coupling reactions.^{9,10} As a testimony of SPO potential in catalysis, Cramer described recently a nickel-based catalytic system including a chiral diaminophosphine oxide for the enantioselective hydrocarbamoylation of alkenes.¹¹ As well, these ligands were also successfully applied to gold-catalyzed cycloisomerization of enynes.¹² On the other hand, it has been demonstrated that PAs were more than phosphine mimics, as they promote an unusual palladium-mediated [2+1] cycloaddition between activated C–C double bonds (norbornene derivatives) and terminal alkynes.¹³ Platinum-based complexes have shown a similar catalytic behavior, and even an unprecedented intermolecular tandem [2+1]/[3+2] cycloaddition sequence was achieved.¹⁴

Received: December 18, 2014

Scheme 2. Preparation of $[\text{RuCl}_2(\text{CO})_3(\text{SPO})]$ Complexes^a

^aAd = adamantyl; NR = no reaction.

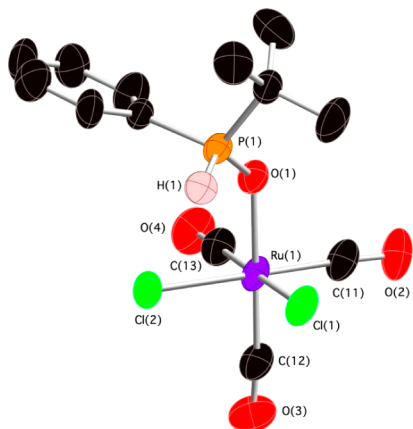


Figure 2. Molecular structure of complex **5a** represented at the 50% ellipsoid probability level. Most of the H atoms have been omitted for clarity. Selected bond lengths (Å) and angles (deg): Ru(1)–O(1) 2.103(5); Ru(1)–C(11) 1.890(9); Ru(1)–C(12) 1.891(9); Ru(1)–C(13) 1.899(10); Ru(1)–Cl(1) 2.398(2); Ru(1)–Cl(2) 2.3853(17); O(1)–P(1) 1.513(5); P(1)–H(1) 1.4895; C(11)–Ru(1)–O(1) 89.1(3); C(11)–Ru(1)–C(12) 92.1(4); C(11)–Ru(1)–C(13) 94.3(4); C(11)–Ru(1)–Cl(1) 85.7(3); Cl(1)–Ru(1)–Cl(2) 91.17(8); Ru(1)–O(1)–P(1) 129.8(3); O(1)–P(1)–H(1) 122.7.

It is noteworthy that, when the two substituents of the phosphorus atom are different, this center becomes stereogenic and does not racemize during the tautomeric equilibrium. Thus, chiral SPOs were successfully applied in asymmetric catalysis.^{13c,15}

In spite of interesting applications of ruthenium-SPO catalytic systems, such as C–H activation,¹⁶ hydrogenation,¹⁷ and nitrile hydration,¹⁸ the preparation of well-defined ruthenium complexes bearing SPO or PA ligands has been barely investigated. Few $[\text{Ru}(\eta^6\text{-arene})(\text{R}^1\text{R}^2\text{POH})]$ complexes **1** or **2** have been reported (Figure 1).^{18–20} Stephenson reported a complex **3** containing a polydentate ligand composed from two PAs and one phosphinito species.²¹ Another study on cyclopentadiene ruthenium species highlighted the difficulty to prepare and isolate well-defined complexes bearing SPO and PA ligands.²²

Herein, we disclose a general study on the coordination mode of SPO and PA ligands to ruthenium. Two series of ruthenium carbonyl complexes bearing either one SPO ligand or two PAs have been synthesized and fully characterized. The catalytic behavior of these complexes has been investigated for the cycloisomerizations of arenynes.

RESULTS AND DISCUSSION

After the examination of several ruthenium sources,²³ we focused our efforts on the commercially available tricarbonyldichlororuthenium(II) dimer. The treatment of $[\text{RuCl}_2(\text{CO})_3]_2$ with 1 equiv of Ph*t*BuPHO **4a** in THF at

room temperature was monitored by ³¹P NMR spectroscopy and showed the rapid appearance of a new resonance at 57.4 ppm with a ¹J(P,H) = 504.6 Hz, whereas the free SPO presents a higher field signal at 47.4 ppm with a ¹J(P,H) = 452.8 Hz. The complex was isolated as an air-stable pale yellow solid in an almost quantitative yield (Scheme 2). The ¹J(P,H) coupling constant indicates that the phosphorus atom is tetracoordinated; thus in **5a**, the ruthenium binds the SPO through the oxygen. To unambiguously establish the structure of **5a**, suitable crystals for single-crystal diffraction studies were obtained. The thermal ellipsoid representation with selected bond distances and angles is presented in Figure 2. **5a** shows

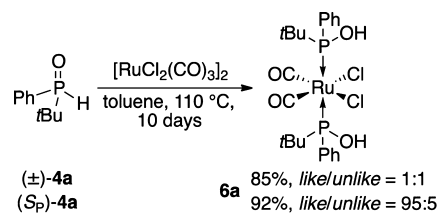
Table 1. ³¹P Chemical Shifts and *J*-Coupling of Complexes **5** and Free SPOs in CDCl₃ at 25 °C

entry	R ¹ , R ²	δ (ppm) (¹ J(P,H) (Hz))	
		complex 5	free SPO 4
1	Ph, <i>t</i> Bu (a)	57.36 (504.6)	47.41 (452.8)
2	Ph, <i>n</i> Bu (b)	43.70 (515.5)	27.98 (463.1)
3	Ph, Me (c)	61.20 (483.4)	49.97 (433.8)
4	Cy, Cy (e)	37.42 (534.0)	20.21 (472.2)

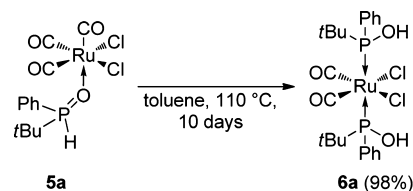
Table 2. Carbonyl and P=O Stretching Frequencies of Complexes **5** (IR Spectra Recorded Using an ATR Device)

entry	complex	ν _{CO} (cm ⁻¹)	ν _{PO} (cm ⁻¹)
1	5a	2130, 2069, 2025	1139
2	5b	2130, 2043	1134
3	5c	2134, 2067, 2049	1136
4	5e	2129, 2044, 1993	1097

Scheme 3. Synthesis of Complex $[\text{RuCl}_2(\text{CO})_2(\text{Ph}t\text{BuPOH})_2]$ **6a**



Scheme 4. Preparation of **6a** Starting from Complex $[\text{RuCl}_2(\text{CO})_3(\text{Ph}t\text{BuPHO})]$, **5a**



the expected distorted octahedral geometry around the metal center with bond angles between 85.7° and 94.3°. The Ru(1)–O(1) distance (2.103 Å) suggests a dative covalent bond, whereas the short O(1)–P(1) bond length (1.513 Å) is in agreement with a double-bond character. Other bond distances were found comparable to those reported for similar complexes.

We prepared other complexes **5** using different SPOs (Scheme 2). Whereas SPOs **4b**, **4c**, and **4e** gave quantitatively the corresponding complexes, no reaction was observed with sterically demanding SPO **4h** and **4i** despite a prolonged

Table 3. Preparation of Complexes $[\text{RuCl}_2(\text{CO})_2(\text{PA})_2]$ **6**

entry	SPO ligand	complex	time (days)	yield (%)	e.d. (%) ^a
1	(±)-Ph <i>t</i> BuPHO, (±)- 4a	6a	10	85	0
2	(<i>S_p</i>)-Ph <i>t</i> BuPHO, (<i>S_p</i>)- 4a	6a	10	92	90
3	(±)-Ph <i>n</i> BuPHO, (±)- 4b	6b	3	82	20
4	(±)-PhMePHO, (±)- 4c	6c	3	30	20
5	(±)-PhCyPHO, (±)- 4d	6d	3	81	20
6	Cy ₂ PHO, 4e	6e	3	92	
7	Ph ₂ PHO, 4f	6f	3	53	
8	(<i>p</i> -F-C ₆ H ₄) ₂ PHO, 4g	6g	3	83	
9	<i>t</i> Bu ₂ PHO, 4h	6h	10	NR ^c	
10 ^b	Ad ₂ PHO, 4i	6i	10	NR	

^ae.d. refers to *like/unlike* ratio. ^bAd = adamantyl. ^cNR = no reaction.

Table 4. Stretching Frequencies of Complexes **6** (IR Spectra Recorded Using an ATR Device)

entry	complex	ν_{CO} (cm ⁻¹)	$\nu_{\text{P-O}}$ (cm ⁻¹)	$\nu_{\text{O-H}}$ (cm ⁻¹)
1	6a , [RuCl ₂ (CO) ₂ (Ph <i>t</i> BuPOH) ₂]	2050, 1993	873	3221
2	6b , [RuCl ₂ (CO) ₂ (Ph <i>n</i> BuPOH) ₂]	2056, 1992	876	3163
3	6d , [RuCl ₂ (CO) ₂ (PhCyPOH) ₂]	2050, 1990	873	3250 (br)
4	6e , [RuCl ₂ (CO) ₂ (Cy ₂ POH) ₂]	2048, 1991	856	3266
5	6f , [RuCl ₂ (CO) ₂ (Ph ₂ POH) ₂]	2058, 1991	879	3100 (br)
6	6g , [RuCl ₂ (CO) ₂ (<i>p</i> -F-C ₆ H ₄) ₂ POH) ₂]	2065, 2002	879	3171

heating at 80 °C in dioxane. ³¹P NMR spectra of the complexes **5b**, **5c**, and **5e** showed a characteristic low-field resonance with a shift from 10 to 17 ppm compared to the free SPO ligands (Table 1). These low values expressed a weak interaction between the ligand and the metal. In the same manner, *J*-couplings increased slightly, from about 50 Hz, and revealed a more pronounced *s* character of the P–H bond.²⁴

By examining the P=O stretching frequencies, we confirmed the coordination of the ligand to the ruthenium through the oxygen atom (Table 2).²⁵ For complex **5a**, a band at 2374 cm⁻¹ relative to the P–H bond stretching frequency was even detected.

We then treated the [RuCl₂(CO)₃]₂ dimer with 4 equiv of SPO **4a** under harsher reaction conditions (toluene at 110 °C) (Scheme 3). The ³¹P NMR monitoring showed the appearance of new resonances at 113.0 and 113.8 ppm. After 10 days, **6a** was isolated in 85% yield as an air- and moisture-stable light yellow solid. We attributed the two resonances to the formation of a 1:1 mixture of diastereomers *like* (*S_p***S_p**) and *unlike* (*R_p***S_p**), resulting from the use of the racemic SPO (±)-**4a**.²⁶ To confirm this hypothesis, the reaction was carried out with the enantiopure SPO (*S_p*)-**4a**, and almost exclusively the diastereomer *like* (*S_p**S_p*) was formed in 92% yield (Scheme 3). It also evidenced that the P-stereogenic center is configurationally stable since only a slight racemization was observed despite the harsh reaction conditions. The NMR monitoring of **6a** synthesis showed an early formation of **5a**, which was suspected to be an intermediate. Indeed, the heating of complex **5a** in toluene for 10 days gave rise to **6a** quantitatively; the yield is based on phosphorus species (Scheme 4).²⁷ However, we were unable to determine if the coordination of the second phosphinous acid by CO displacement occurred before or after the already bound SPO ligand switches its coordination mode.

The preparation of a series of complexes **6** was then achieved using various dissymmetric and symmetric SPO preligands (Table 3). Complexes **6** were isolated in moderate to good yields, except for **6c**, which presented a low stability (30%, entry 4). Bulky phosphinous acids, such as *t*Bu₂POH **4h** and Ad₂POH **4i**, were unable to coordinate the ruthenium center despite a prolonged heating at 110 °C (entries 9 and 10). With racemic dissymmetric SPOs **4b–d**, low diastereoselectivities were observed, and the relative configurations of the major diastereomers could not be attributed (entries 3–5). The quantification of the steric parameter of phosphinous acids through the percent buried volume (%*V*_{bur})^{28,29} has been previously determined on gold complexes.¹² It revealed that *t*Bu₂POH is significantly more sterically demanding than *t*BuPhPOH (32.6% vs 29.2%) and might explain the absence of coordination we noticed.

The IR stretching frequencies of complexes **6** allowed us to collect structural information (Table 4). The $\nu_{\text{P-O}}$ and $\nu_{\text{O-H}}$ bands in the ranges 856–879 cm⁻¹ and 3100–3266 cm⁻¹, respectively, confirmed the formation of Ru–P bonds. Moreover, the two ν_{CO} bands at 2050–2065 cm⁻¹ and 1990–2002 cm⁻¹ indicated a *cis* arrangement of the carbonyl

Table 5. Selected Bond Lengths (Å) and Angles (deg) for Complexes [RuCl₂(CO)₂(PA)₂] **6a**, **6c**, and **6e**

entry	complex	Ru–P (Å)	Ru–C (Å)	Ru–Cl (Å)	P–O (Å)	O...Cl (Å)
1	6a	2.4050(6)	1.860(2)	2.4399(6)	1.6016(17)	3.048
		2.4060(7)	1.863(2)	2.4404(6)	1.5995(17)	3.051
2	6d	2.3919(18)	1.863(7)	2.4306(16)	1.607(4)	2.983
		2.3940(19)	1.856(7)	2.4274(17)	1.603(5)	3.077
2	6e	2.3988(9)	1.892(15)	2.400(4)	1.612(2)	3.036
		2.4045(8)	1.893(13)	2.424(4)	1.616(2)	3.226
entry	complex	P–Ru–P (deg)	C–Ru–C (deg)	Cl–Ru–Cl (deg)		
4	6a	164.50(2)	91.37(11)	88.55(2)		
5	6d	170.34(6)	92.7(3)	88.04(6)		
6	6e	180.00(4)	90.6(9)	83.03(17)		

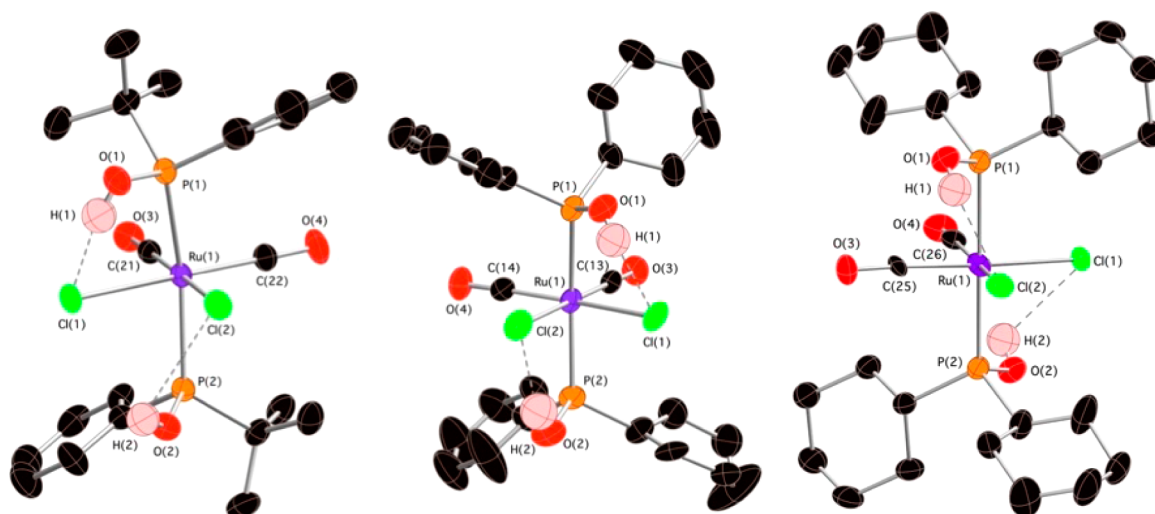


Figure 3. Molecular structures of complexes **6a** (left), **6d** (middle), and **6e** (right) represented at 50% ellipsoid probability. Most of the H atoms have been omitted for clarity.

groups. Indeed, for $[\text{RuCl}_2(\text{CO})_2(\text{PPh}_3)_2]$, the *trans* arrangement of the CO ligands is characterized by a single asymmetric stretching band at 2011 cm^{-1} , whereas the *cis* configuration shows symmetric and asymmetric stretching bands at 2059 and 1997 cm^{-1} .³⁰ The CO symmetric stretching frequencies of complexes **6** allowed the ranking of PA ligands according to their σ -donating properties, Cy_2POH being the most electron-donating ligand and $(p\text{-F-C}_6\text{H}_4)_2\text{POH}$ the least. This is in good agreement with Tolman's seminal work.³¹ In this series, the difference of electronic properties between phosphinoyl acids and phosphines was found to be small (2058 cm^{-1} for Ph_2POH vs 2059 cm^{-1} for PPh_3).

A single-crystal X-ray diffraction study was performed to unambiguously determine the atom connectivity in complexes **6a**, **6d**, and **6e**. ORTEP representations are shown in Figure 3, and selected bond lengths and angles are reported in Table 5. The ruthenium atom adopted an octahedral geometry around the metal center in all the complexes with *cis* arrangements of chlorines and carbonyls. PAs were positioned in *trans* position with a hydrogen bonding with chlorines, attested by $\text{O}\cdots\text{Cl}$ distances less to 3.2 \AA . The P-Ru-P angle for **6a** (164.50°) indicated a tilt probably to accommodate both the steric bulk of PhfBuPOH and the hydrogen bondings. Other bond distances and angles were similar to those reported for analogous complexes.

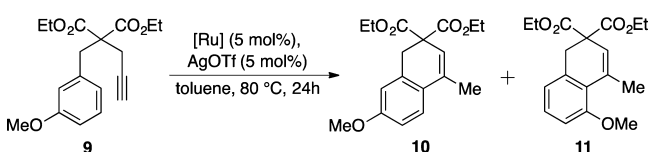
As Murai reported that $[\text{RuCl}_2(\text{CO})_3]_2$ was a versatile catalyst for the cycloisomerization of arenynes,³² we decided to evaluate the performances of the new complexes **5** and **6** in this transformation. Arenyne **7**, with an electron-rich aryl, was first selected as a benchmark substrate (Table 6). Under the optimized reaction conditions (16 mol % of Ru, 16% of AgOTf , in toluene at $25\text{ }^\circ\text{C}$), control experiments showed that $[\text{RuCl}_2(\text{CO})_3]_2$ was ineffective (entries 1 and 2). Low conversions were observed with the silver salt alone and with catalyst **5a** (entries 3 and 4). We were pleased to see that better conversions were achieved with complexes **6**.³³ Whereas **6a** and **6g** gave moderate transformation rates (entries 5 and 9), much better activities were reached with catalysts **6d**, **6f**, and especially **6e**, bearing the more electron-rich PA ligands (entries 6–8). Thus, the catalyst loading could be reduced down to 2 mol % with a slight increase of the reaction duration to complete the cycloisomerization (entries 10–13).

Table 6. Cycloisomerization of Arenyne **7**^a

entry	[Ru]	loading (mol %)	time (h)	conversion (%) ^b
1	$[\text{RuCl}_2(\text{CO})_3]_2$	8 (16 mol % Ru)	3	traces
2 ^c	$[\text{RuCl}_2(\text{CO})_3]_2$	8 (16 mol % Ru)	3	traces
3 ^d	none	16	3	15
4	5a , $[\text{RuCl}_2(\text{CO})_3(\text{PhfBuPHO})]$	16	3	11
5	6a , $[\text{RuCl}_2(\text{CO})_2(\text{PhfBuPOH})_2]$	16	1	50
6	6d , $[\text{RuCl}_2(\text{CO})_2(\text{PhCyPOH})_2]$	16	1	90
7	6e , $[\text{RuCl}_2(\text{CO})_2(\text{Cy}_2\text{POH})_2]$	16	0.5	100 (77) ^e
8	6f , $[\text{RuCl}_2(\text{CO})_2(\text{Ph}_2\text{POH})_2]$	16	1	83
9	6g , $[\text{RuCl}_2(\text{CO})_2(p\text{-F-C}_6\text{H}_4)_2\text{POH})_2]$	16	3	64
10	6e , $[\text{RuCl}_2(\text{CO})_2(\text{Cy}_2\text{POH})_2]$	8	1	100
11	6e , $[\text{RuCl}_2(\text{CO})_2(\text{Cy}_2\text{POH})_2]$	5	1	95
12	6e , $[\text{RuCl}_2(\text{CO})_2(\text{Cy}_2\text{POH})_2]$	2	1	38
13	6e , $[\text{RuCl}_2(\text{CO})_2(\text{Cy}_2\text{POH})_2]$	2	8	100

^aReaction conditions: $[\text{Ru}]/\text{AgOTf}$, 1:1, **7** (0.5 mmol), toluene (2.5 mL, 0.2 M), $25\text{ }^\circ\text{C}$. ^bConversions determined by $^1\text{H NMR}$. ^cWithout silver salt. ^dOnly AgOTf was used. ^eIsolated yield.

We also scrutinized a less activated arenyne **9** bearing only one methoxy group on the aryl moiety; the reaction mixture required a thermal activation at $80\text{ }^\circ\text{C}$ to form products **10** and **11** (Table 7). Due to the steric congestion caused by the methoxy, isomer **10** is mainly detected, and the catalyst used does not seem to influence this selectivity. Surprisingly, catalysts **6a** and **6f** exhibited a significantly better activity than **6d** and **6e** (entries 1–4). Whereas **6a** and **6d** presented similar stretching frequencies (Table 4), the higher catalytic of **6a** over **6d** is certainly due to the difference in steric congestion. In general, the trend observed with this substrate is the

Table 7. Cycloisomerization of Arenyne **9**^a

entry	[Ru]	AgX	conversion (%) ^b	10/11 ratio ^b
1	6a , [RuCl ₂ (CO) ₂ (PhfBuPOH) ₂]	AgOTf	99	97:3
2	6d , [RuCl ₂ (CO) ₂ (PhCyPOH) ₂]	AgOTf	45	95:5
3	6e , [RuCl ₂ (CO) ₂ (Cy ₂ POH) ₂]	AgOTf	35	96:4
4	6f , [RuCl ₂ (CO) ₂ (Ph ₂ POH) ₂]	AgOTf	99	97:3
5	6a , [RuCl ₂ (CO) ₂ (PhfBuPOH) ₂]	AgBF ₄	NR ^c	
6	6a , [RuCl ₂ (CO) ₂ (PhfBuPOH) ₂]	AgOAc	NR	
7	6a , [RuCl ₂ (CO) ₂ (PhfBuPOH) ₂]	AgPF ₆	NR	
8	6a , [RuCl ₂ (CO) ₂ (PhfBuPOH) ₂]	AgSbF ₆	100	85:15

^aReaction conditions: [Ru]/AgOTf, 1:1 (5 mol %), **9** (0.5 mmol), toluene (2.5 mL, 0.2 M), 80 °C, 24 h. ^bDetermined by ¹H NMR. ^cNR = no reaction.

opposite of that with arenynes **7**. This highlighted a strong relationship between ligand and substrate structures and suggested different rate-determining steps.³⁴ In the case of substrate **9**, complexes containing electron-poor ligands (**6a** and **6f**) seemed to activate efficiently the alkyne by an accentuation of the cationic character of the vinyl-ruthenium intermediate and triggers the nucleophilic attack, which was less favored. On the other hand, when the nucleophilic attack was not the rate-determining step, for the activated arenynes **7**, electron-rich ligands might boost the demetalation process.

In this study, we also noticed a drastic effect of the silver salt used. Whereas AgOTf and AgSbF₆ performed well, no reaction was observed with AgBF₄, AgOAc, or AgPF₆ (entries 1 and 5–7). A similar observation was recently reported by Bour and Gandon for gallium complexes.³⁵ According to their observations with anions BF₄ and PF₆, the chlorine abstraction from the metallic center was followed by a fluorine transfer to the metal, while SbF₆ is stable enough to prevent this transfer. The lack of reactivity noticed with AgOAc is in agreement with the higher coordination capacity of the counteranion OAc that decreases the Lewis acid character of Ag(I).³⁶

CONCLUSION

To summarize, we studied the coordination chemistry of secondary phosphine oxides and phosphinous acids with [RuCl₂(CO)₃]₂ and achieved the preparation of two series of ruthenium complexes. It was found that SPOs could bind ruthenium through the oxygen atom to give rare and stable SPO-metal complexes, which were fully characterized. On the other hand, the modification of the reaction conditions led to the formation of another series of complexes bearing two PA ligands. The complete characterization of these complexes enabled the determination of PAs' electronic parameter. Their reactivity was evaluated in the cycloisomerization of arenynes with two benchmark substrates. It was noticed a strong ligand effect and a relationship between the ligand electronic parameter and the structure of the substrates that can be explained by an influence on two distinct rate-determining

steps. We hope this study will contribute to the better understanding of the coordination chemistry of SPO and PA ligands and will enhance their use to develop new catalytic systems.

EXPERIMENTAL SECTION

General Information. All reactions were performed under an argon atmosphere. All reagents were obtained from commercial sources and used as received. SPO ligands **4** were obtained from a chemical supplier or by following literature procedures.³⁷ Solvents (THF and toluene) were purified and dried over a Braun solvent purification system (MB-SPS-800). Analytical thin layer chromatography (TLC) was carried out on Merck silica gel 60 F₂₅₄. Products were revealed by ultraviolet light (254 or 366 nm) and stained with dyeing reagent solutions as a 5% phosphomolybdic acid solution, potassium permanganate solution, or *p*-anisaldehyde solution in ethanol followed by gentle heating. Flash chromatography purifications were performed on Combiflash Companion or with Merck silica gel 60 (230–400 mesh). ¹H, ¹³C, ³¹P, and ¹⁹F NMR spectra were recorded in CDCl₃ at ambient temperature on Bruker Avance III 300 or 400 spectrometers operating at 300 and 400 MHz, respectively for ¹H, ¹³C, ³¹P, and ¹⁹F nuclei were observed with ¹H decoupling. Solvent residual signals were used as internal standard. Chemical shifts (δ) and coupling constants (*J*) are given in ppm and Hz, respectively. The peak patterns are indicated in the following format: multiplicity (s: singlet; d: doublet; t: triplet; q: quartet; sept: septuplet; m: multiplet; dd: doublet of doublets; dt: doublet of triplets; dm: doublet of multiplets, etc.). The prefix br indicates a broadened signal. Infrared spectra were recorded on a Bruker VERTEX70 Fourier transform infrared spectrometer equipped with a single reflection diamond attenuated total reflectance (ATR) Bruker A222 accessory. IR data are reported as characteristic bands (cm⁻¹). Elemental analyses were performed on a Thermo Finnigan EA 1112 analyzer. HRMS were recorded on a SYNAPT G2 HDMS (Waters) or on a QStar Elite (Applied Biosystems SGIEX) equipped with an atmospheric pressure ionization (API) source. Mass spectra were obtained a time of flight (TOF) analyzer. Intensity data were collected on a Bruker-Nonius KappaCCD diffractometer using graphite-monochromated Mo K α radiation (0.71073 Å) at 293(2) K. The collected frames were processed with the software HKL-2000, and structures were resolved by the direct methods and refined using the SHELXL-97 software package.

General Procedure for the Synthesis of Complexes [RuCl₂(CO)₃(R¹R²PHO)]. In a Schlenk flask, under argon, charged with [RuCl₂(CO)₃]₂ (102 mg, 0.2 mmol), a solution of ligand SPO **4** (0.4 mmol, 2 equiv) in THF (4 mL, 0.1 M) was added. The reaction mixture was stirred for 2 h at room temperature. The solvent was removed under vacuum. The crude mixture was solubilized in dichloromethane and precipitated in *n*-hexane. The solid was filtered, washed with *n*-hexane, and dried under vacuum to give the desired product.

[RuCl₂(CO)₃(*t*BuPhPHO)] (5a**).** According to the general procedure, **5a** was prepared from SPO *t*BuPhPHO **4a** and obtained as a white solid (151 mg, 87%). ¹H NMR (400 MHz, CDCl₃): δ (ppm) = 7.70–7.50 (m, 5H, H^{Ar}), 7.50 (d, ¹J(H,P) = 504.6 Hz, 1H, P-H), 1.17 (d, ¹J(H,P) = 17.5 Hz, 9H, CH₃). ¹³C{¹H} NMR (101 MHz, CDCl₃): δ (ppm) = 187.3 (CO), 184.0 (CO), 133.5 (d, ⁴J(C,P) = 2.9 Hz, C^{Ar}-H), 130.9 (d, ¹J(C,P) = 10.7 Hz, C^{Ar}-H), 129.1 (d, ¹J(C,P) = 12.5 Hz, C^{Ar}-H), 126.1 (d, ¹J(C,P) = 94.8 Hz, C^{Ar}-P), 31.2 (d, ¹J(C,P) = 70.7 Hz, C), 24.0 (d, ²J(C,P) = 2.2 Hz, CH₃). ³¹P NMR (162 MHz, CDCl₃): δ (ppm) = 57.4 (dm, ¹J(H,P) = 504.6 Hz). HRMS (ESI+): *m/z* calcd for C₁₃H₁₉Cl₂NO₄PRu 455.9464 [M + NH₄]⁺; found 455.9471. IR (ATR, diamond crystal): 2979, 2374 (P-H), 2129 (CO), 2069 (CO), 2025 (CO), 1590, 1475, 1437, 1369, 1139 (P=O), 1106, 905. Anal. Calcd for C₁₃H₁₅Cl₂O₄PRu: C, 35.63; H, 3.45. Found: C, 35.29; H, 3.27.

[RuCl₂(CO)₃(*n*BuPhPHO)] (5b**).** According to the general procedure, **5b** was prepared from SPO *n*BuPhPHO **4b** and obtained as a white solid (162 mg, 93%). ¹H NMR (400 MHz, CDCl₃): δ (ppm) = 7.90 (dt, ¹J(H,P) = 515.5 Hz, ¹J(H,H) = 3.6 Hz, 1H, P-H), 7.75–7.50 (m,

5H, H^{Ar}), 2.31–2.23 (m, 2H, P-CH₂), 1.55–1.37 (m, 4H, 2 CH₂), 0.89 (t, J(H,H) = 7.1 Hz, 3H, CH₃). ¹³C{¹H} NMR (75 MHz, CDCl₃): δ (ppm) = 187.2 (d, ³J(C,P) = 1.6 Hz, CO), 183.6 (d, ³J(C,P) = 6.3 Hz, CO), 133.4 (d, ⁴J(C,P) = 2.8 Hz, C^{Ar}-H), 130.5 (d, J(C,P) = 11.5 Hz, C^{Ar}-H), 129.3 (d, J(C,P) = 13.0 Hz, C^{Ar}-H), 126.9 ((d, J(C,P) = 102.4 Hz, C^{Ar}), 28.1 (d, ¹J(C,P) = 68.1 Hz, P-CH₂), 23.5 (d, ²J(C,P) = 15.6 Hz, CH₂), 23.1 (d, ³J(C,P) = 3.1 Hz, CH₂), 13.4 (s, CH₃). ³¹P NMR (162 MHz, CDCl₃): δ (ppm) = 43.7 (dm, ¹J(H,P) = 515.5 Hz). HRMS (ESI+): *m/z* calcd for C₁₃H₁₅Cl₂NaO₄PRu 460.9018 [M + Na]⁺; found 460.9022. IR (ATR, diamond crystal): 2130 (CO), 2043 (CO), 1597, 1439, 1134 (P=O), 1089, 935, 691, 618, 475. Anal. Calcd for C₁₃H₁₅Cl₂O₄PRu: C, 35.63; H, 3.45. Found: C, 35.39; H, 3.31.

[RuCl₂(CO)₃(MePhPHO)] (**5c**). According to the general procedure, **5c** was prepared from SPO MePhPHO **4c** and obtained as a yellow solid (143 mg, 90%). ¹H NMR (400 MHz, CDCl₃): δ (ppm) = 8.05 (dq, ¹J(H,P) = 534.0 Hz, J(H,H) = 4.1 Hz, 1H, P-H), 7.80–7.50 (m, 5H, H^{Ar}), 2.03 (dd, ²J(H,P) = 13.8 Hz, J(H,H) = 4.1 Hz, 3H, CH₃). ¹³C{¹H} NMR (75 MHz, CDCl₃): δ (ppm) = 187.2 (d, ³J(C,P) = 1.8 Hz, CO), 183.5 (d, ³J(C,P) = 3.0 Hz, CO), 133.6 (d, ⁴J(C,P) = 2.9 Hz, C^{Ar}-H), 130.4 (d, J(C,P) = 12.0 Hz, C^{Ar}-H), 129.3 (d, J(C,P) = 13.3 Hz, C^{Ar}-H), 127.9 (d, J(C,P) = 106.8 Hz, C^{Ar}), 15.2 (d, ¹J(C,P) = 70.0 Hz, CH₂). ³¹P NMR (162 MHz, CDCl₃): δ (ppm) = 37.4 (dq, ¹J(H,P) = 534.0 Hz, ²J(H,P) = 13.7 Hz). HRMS (ESI): *m/z* calcd for C₁₀H₉Cl₂NaO₄PRu 418.8548 [M + Na]⁺; found 418.8549. IR (ATR, diamond crystal): 2134 (CO), 2067 (CO), 2049 (CO), 1587, 1437, 1406, 1301, 1136 (P=O), 1071, 961. Anal. Calcd for C₁₀H₉Cl₂O₄PRu: C, 30.32; H, 2.29. Found: C, 29.98; H, 2.10.

[RuCl₂(CO)₃(Cy₂PHO)] (**5e**). According to the general procedure, **5e** was prepared from SPO Cy₂PHO **4e** and obtained as a white solid (182 mg, 97%). ¹H NMR (400 MHz, CDCl₃): δ (ppm) = 6.76 (d, ¹J(H,P) = 483.7 Hz, 1H, P-H), 2.10–1.10 (complex multiplet, 22H, CH and CH₂). ¹³C{¹H} NMR (75 MHz, CDCl₃): δ (ppm) = 187.3 (d, ³J(C,P) = 1.7 Hz, CO), 184.0 (br s, CO), 34.5 (d, ¹J(C,P) = 63.9 Hz, CH), 26.3 (s, CH₂), 26.3 (br s, CH₂), 26.1 (br s, CH₂), 25.7 (d, J(C,P) = 1.5 Hz, CH₂), 25.6 (d, J(C,P) = 3.0 Hz, CH₂). ³¹P NMR (121 MHz, CDCl₃): δ (ppm) = 61.2 (dm, ¹J(H,P) = 483.4 Hz). HRMS (ESI): *m/z* calcd for C₁₅H₂₃Cl₂NaO₄PRu 492.9645 [M + Na]⁺; found 492.9663. IR (ATR, diamond crystal): 2928, 2854, 2129 (CO), 2044 (CO), 1993 (CO), 1449, 1097 (P=O), 620. Anal. Calcd for C₁₅H₂₃Cl₂O₄PRu: C, 38.31; H, 4.93. Found: C, 38.66; H, 4.89.

General Procedure for the Preparation of Complexes [RuCl₂(CO)₂(R¹R²POH)]₂. In a Schlenk flask, under argon, charged with [RuCl₂(CO)₃]₂ (102 mg, 0.2 mmol), a solution of preligand SPO **4** (0.88 mmol, 4.4 equiv) in toluene (4 mL, 0.1 M) was added. The reaction mixture was stirred from 3 to 10 days at 110 °C. The solvent was removed under vacuum. The crude mixture was filtered over a pad of silica gel, eluted by DCM, and dried under vacuum to give the desired product.

[RuCl₂(CO)₂(*t*BuPhPHO)]₂, **6a-like**. According to the general procedure, **6a** was prepared from SPO (S_p)-(*t*BuPhPHO), (S_p)-**4a**, and obtained as a light yellow solid (216 mg, 92%) as a mixture of *like* and *unlike* compounds (de = 90%). ¹H NMR (400 MHz, CDCl₃): δ (ppm) = 7.74–7.64 (m, 4H, H^{Ar}), 7.52–7.44 (m, 6H, H^{Ar}), 6.94 (s, 2H, PO-H), 1.23 (d, J(H,P) = 8.3 Hz, 9H, 3 CH₃), 1.21 (d, J(H,P) = 8.1 Hz, 9H, 3 CH₃). ¹³C{¹H} NMR (101 MHz, CDCl₃): δ (ppm) = 194.1 (t, ²J(C,P) = 10.9 Hz, CO), 134.1 (t, ¹J(C,P) = 25.2 Hz, C^{Ar}), 130.9 (br s, C^{Ar}-H), 130.1 (t, J(C,P) = 5.9 Hz, C^{Ar}-H), 128.3 (t, J(C,P) = 5.1 Hz, C^{Ar}-H), 38.6 (t, ¹J(C,P) = 16.4 Hz, C), 25.4 (t, ²J(C,P) = 2.6 Hz, CH₂). ³¹P{¹H} NMR (162 MHz, CDCl₃): δ (ppm) = 113.9 (s). HRMS (ESI+): *m/z* calcd for C₂₂H₃₀Cl₂NaO₄P₂Ru 614.9932 [M + Na]⁺; found 614.9930. IR (ATR, diamond crystal): 3221 (OH), 2981, 2935, 2906, 2873, 2050 (CO), 1993 (CO), 1960, 1438, 1368, 1131, 873 (P-O), 697, 608, 513. Anal. Calcd for C₂₂H₃₀Cl₂O₄P₂Ru: C, 44.60; H, 5.10. Found: C, 44.78; H, 4.99.

[RuCl₂(CO)₂(*t*BuPhPHO)]₂, **6a-unlike**. According to the general procedure, **6a** was prepared from SPO (±)-*t*BuPhPHO, (±)-**4a**, and obtained as a light yellow solid (206 mg, 85%) as a mixture of *like* and *unlike* compounds (de = 0%). ¹H NMR (400 MHz, CDCl₃): δ (ppm) = 7.68–7.60 (m, 4H, H^{Ar}), 7.47–7.40 (m, 6H, H^{Ar}), 6.94 (s, 2H, PO-

H), 1.27 (d, J(H,P) = 8.4 Hz, 9H, 3 CH₃), 1.25 (d, J(H,P) = 7.8 Hz, 9H, 3 CH₃). ³¹P{¹H} NMR (162 MHz, CDCl₃): δ (ppm) = 113.0 (s).

[RuCl₂(CO)₂(*n*BuPhPHO)]₂, **6b**. According to the general procedure, **6b** was prepared from SPO (±)-*n*BuPhPHO, (±)-**4b**, and was obtained as a yellow solid (201 mg, 85%) as a mixture of *like* and *unlike* compounds (de = 20%). ¹H NMR (400 MHz, CDCl₃): δ (ppm) = 7.70–7.30 (m, 10H, H^{Ar}), 5.00 (br s, PO-H), 2.84 (m, 2.3H, CH₂), 2.15 (m, 2H, CH₂), 1.70–1.15 (m, 8.5H, CH₂), 0.86 (t, J(H,H) = 7.2 Hz, 2.3H, CH₃), 0.83 (t, J(H,H) = 7.2 Hz, 3.7H, CH₃). ¹³C{¹H} NMR (101 MHz, CDCl₃): δ (ppm) = 191.8 (t, ²J(C,P) = 11.4 Hz, CO), 136.3 (t, J(C,P) = 27.1 Hz, C^{Ar}, major), 135.7 (t, J(C,P) = 27.8 Hz, C^{Ar}, minor), 131.0 (br s, C^{Ar}-H), 129.1 (t, J(C,P) = 5.1 Hz, C^{Ar}-H, major), 128.9 (t, J(C,P) = 5.5 Hz, C^{Ar}-H, minor), 128.8 (t, J(C,P) = 6.2 Hz, C^{Ar}-H, minor), 128.6 (t, J(C,P) = 6.6 Hz, C^{Ar}-H, major), 33.0 (t, J(C,P) = 17.6 Hz, CH₂-P, minor), 32.5 (t, J(C,P) = 18.0 Hz, CH₂-P, major), 23.9 (m, CH₂), 13.7 (m, CH₃). ³¹P{¹H} NMR (162 MHz, CDCl₃): δ (ppm) = 104.8 (s, minor), 103.7 (s, major). HRMS (ESI+): *m/z* calcd for C₂₂H₃₄Cl₂NO₄P₂Ru 610.0378 [M + NH₄]⁺; found 610.0383. IR (ATR, diamond crystal): 3163 (OH), 2958, 2931, 2870, 2056 (CO), 1992 (CO), 1436, 1109, 876 (P-O), 743, 692, 577. Anal. Calcd for C₂₂H₃₀Cl₂O₄P₂Ru: C, 44.61; H, 5.10. Found: C, 44.77; H, 5.22.

[RuCl₂(CO)₂(MePhPHO)]₂, **6c**. According to the general procedure, **6c** was prepared from SPO (±)-MePhPHO, (±)-**4c**, and obtained as a yellow oil (61 mg, 30%) as a mixture of *like* and *unlike* compounds (de = 20%). ¹H NMR (400 MHz, CDCl₃): δ (ppm) = 7.70–7.45 (m, 10H, H^{Ar}), 5.39 (br s, P-OH), 2.21 (t, ²J(H,P) = 3.4 Hz, 2.5H, CH₃), 2.18 (t, ²J(H,P) = 3.5 Hz, 3.5H, CH₃). ¹³C{¹H} NMR (101 MHz, CDCl₃): δ (ppm) = 191.5 (t, ²J(C,P) = 11.6 Hz, CO), 138.5 (t, J(C,P) = 28.7 Hz, C^{Ar}, major), 137.9 (t, J(C,P) = 27.1 Hz, C^{Ar}, minor), 131.3 (br s, C^{Ar}-H), 129.2 (t, J(C,P) = 5.2 Hz, C^{Ar}-H, major), 129.0 (t, J(C,P) = 5.3 Hz, C^{Ar}-H, minor), 128.3 (t, J(C,P) = 6.5 Hz, C^{Ar}-H, minor), 128.1 (t, J(C,P) = 6.5 Hz, C^{Ar}-H, major), 19.9 (t, ¹J(C,P) = 19.0 Hz, CH₃, minor), 19.5 (t, J(C,P) = 19.4 Hz, CH₃, major). ³¹P{¹H} NMR (162 MHz, CDCl₃): δ (ppm) = 101.6 (s, minor), 100.6 (s, major). HRMS (ESI+): *m/z* calcd for C₁₆H₁₈Cl₂NaO₄P₂Ru 530.8992 [M + Na]⁺; found 530.8974.

[RuCl₂(CO)₂(CyPhPHO)]₂, **6d**. According to the general procedure, **6d** was prepared from SPO (±)-CyPhPHO, (±)-**4d**, and obtained as a light yellow solid (209 mg, 81%) as a mixture of *like* and *unlike* compounds (de = 20%). ¹H NMR (300 MHz, CDCl₃): δ (ppm) = 7.70–7.40 (m, 10H, H^{Ar}), 7.01 (s, 1H, PO-H, major), 6.72 (s, 1H, PO-H, minor), 2.70–0.80 (m, 22H, CH and CH₂). ¹³C{¹H} NMR (75 MHz, CDCl₃): δ (ppm) = 192.7 (CO), 134.1 (t, ¹J(C,P) = 24.9 Hz, C^{Ar}-P), 133.8 (t, ¹J(C,P) = 26.0, C^{Ar}-P), 131.1 (br s, C^{Ar}-H), 131.0 (br s, C^{Ar}-H), 129.74 (t, J(C,P) = 6.2 Hz, C^{Ar}-H), 129.70 (t, J(C,P) = 6.3 Hz, C^{Ar}-H), 128.6 (t, J(C,P) = 5.1 Hz, C^{Ar}-H), 128.5 (t, J(C,P) = 5.2 Hz, C^{Ar}-H), 42.5 (t, ¹J(C,P) = 17.1 Hz, CH, minor), 41.7 (t, ¹J(C,P) = 17.2 Hz, CH, major), 26.8–26.2 (m, CH₂), 26.1 (br s, CH₂), 25.8 (br s, CH₂, minor), 25.6 (br s, CH₂, major). ³¹P{¹H} NMR (121 MHz, CDCl₃): δ (ppm) = 106.2 (s), 104.9 (s). HRMS (ESI+): *m/z* calcd for C₂₆H₃₄Cl₂NaO₄P₂Ru 667.0247 [M + Na]⁺; found 667.0250. IR (ATR, diamond crystal): 3500–3000, 3250 (OH), 2929, 2856, 2050 (CO), 1990 (CO), 1435, 1111, 873 (P-O), 746, 694, 622, 577. Anal. Calcd for C₂₆H₃₄Cl₂O₄P₂Ru: C, 48.46; H, 5.32. Found: C, 48.60; H, 5.19.

[RuCl₂(CO)₂(Cy₂PHO)]₂, **6e**. According to the general procedure, **6e** was prepared from SPO Cy₂PHO **4e** and obtained as a yellow solid (256 mg, 92%). ¹H NMR (400 MHz, CDCl₃): δ (ppm) = 6.12 (s, 2H, PO-H), 2.48 (m, 4H, P-CH), 2.15–1.20 (m, 40H, 20 CH₂). ¹³C{¹H} NMR (101 MHz, CDCl₃): δ (ppm) = 194.5 (t, ²J(C,P) = 10.8 Hz, CO), 40.6 (J(C,P) = 14.8 Hz, 4 CH), 27.2 (s, CH₂), 27.0 (t, J(C,P) = 6.1 Hz, CH₂), 26.8 (m CH₂), 26.3 (s, CH₂). ³¹P{¹H} NMR (162 MHz, CDCl₃): δ (ppm) = 119.5 (s). HRMS (ESI+): *m/z* calcd for C₂₆H₅₀Cl₂NO₄P₂Ru 674.1632 [M + NH₄]⁺; found 674.1629. IR (ATR, diamond crystal): 3266 (OH), 2929, 2852, 2048 (CO), 1991 (CO), 1953, 1446, 1147, 856 (P-O), 838, 743, 579. Anal. Calcd for C₂₆H₄₆Cl₂O₄P₂Ru: C, 47.56; H, 7.06. Found: C, 47.68; H, 7.00.

[RuCl₂(CO)₂(Ph₂PHO)]₂, **6f**. According to the general procedure, **6f** was prepared from SPO Ph₂PHO **4f** and obtained as a yellow solid

(131 mg, 53%). ^1H NMR (300 MHz, CDCl_3): δ (ppm) = 7.95–7.70 (m, 8 H^{Ar}), 7.60–7.40 (m, 12 H^{Ar}). $^{13}\text{C}\{^1\text{H}\}$ NMR (75 MHz, CDCl_3): δ (ppm) = 192.0 (t, $^2\text{J}(\text{C,P}) = 11.6$ Hz, CO), 135.3 (m, C^{Ar}), 131.6 (br s, $\text{C}^{\text{Ar-H}}$), 130.5 (t, $\text{J}(\text{C,P}) = 6.8$ Hz, $\text{C}^{\text{Ar-H}}$), 128.7 (t, $\text{J}(\text{C,P}) = 5.5$ Hz, $\text{C}^{\text{Ar-H}}$). $^{31}\text{P}\{^1\text{H}\}$ NMR (121 MHz, CDCl_3): δ (ppm) = 94.4 (s). HRMS (ESI+): m/z calcd for $\text{C}_{26}\text{H}_{26}\text{Cl}_2\text{NO}_4\text{P}_2\text{Ru}$ 649.9754 [$\text{M} + \text{NH}_4$] $^+$; found 649.9752. IR (ATR, diamond crystal): 3600–2600, 3100 (OH), 3057, 2922, 2900, 2851, 2136, 2058 (CO), 1991 (CO), 1436, 1101, 879 (P–O), 690, 523. Anal. Calcd for $\text{C}_{26}\text{H}_{22}\text{Cl}_2\text{O}_4\text{P}_2\text{Ru}$: C, 49.38; H, 3.51. Found: C, 49.30; H, 3.32.

$[\text{RuCl}_2(\text{CO})_2(\text{4-fluorophenyl})_2\text{POH}]_2$, **6g**. According to the general procedure, **6g** was prepared from SPO ($p\text{-FC}_6\text{H}_4$) $_2$ PHO **4g** and obtained as a white solid (234 mg, 83%). ^1H NMR (400 MHz, CDCl_3): δ (ppm) = 7.80–7.65 (m, 8H, H^{Ar}), 7.30–7.10 (m, 8H, H^{Ar}). $^{13}\text{C}\{^1\text{H}\}$ NMR (101 MHz, CDCl_3): δ (ppm) = 191.8 (t, $^2\text{J}(\text{C,P}) = 11.4$ Hz, CO), 164.9 (d, $\text{J}(\text{C,F}) = 254$ Hz, C^{Ar}), 133.1 (dd, $\text{J}(\text{C,P}) = 7.8$ Hz, $\text{J}(\text{C,F}) = 16.3$ Hz, C^{Ar}), 130.9 (td, $\text{J}(\text{C,P}) = 31.7$ Hz, $\text{J}(\text{C,F}) = 3.4$ Hz, C^{Ar}), 116.4 (td, $\text{J}(\text{C,P}) = 6.2$ Hz, $\text{J}(\text{C,F}) = 21.8$ Hz, C^{Ar}). $^{31}\text{P}\{^1\text{H}\}$ NMR (162 MHz, CDCl_3): δ (ppm) = 94.3 (s). $^{19}\text{F}\{^1\text{H}\}$ NMR (376 MHz, CDCl_3): δ (ppm) = –106.6 (s). HRMS (ESI+): m/z calcd for $\text{C}_{26}\text{H}_{22}\text{NO}_4\text{P}_2\text{Cl}_2\text{F}_4\text{Ru}$ 721.9377 [$\text{M} + \text{NH}_4$] $^+$; found 721.9382. IR (ATR, diamond crystal): 3171 (OH), 3063, 3101, 2065 (CO), 2002 (CO), 1588, 1498, 1235, 1160, 1105, 879 (P–O), 826, 530. Anal. Calcd for $\text{C}_{26}\text{H}_{18}\text{Cl}_2\text{F}_4\text{O}_4\text{P}_2\text{Ru}$: C, 44.34; H, 2.58. Found: C, 44.68; H, 2.86.

■ ASSOCIATED CONTENT

Supporting Information

Experimental procedures, ^1H , ^{13}C , $^{31}\text{P}\{^1\text{H}\}$, and $^{19}\text{F}\{^1\text{H}\}$ NMR spectra. Crystallographic information files (CIF) for all XRD structures (**5a**, **6a**, **6d**, and **6e**, CCDC 1024151–1024155, respectively), which can also be obtained from the Cambridge Crystallographic Data Centre via www.ccdc.cam.ac.uk/data_request/cif. The Supporting Information is available free of charge on the ACS Publications website at DOI: 10.1021/om501300p.

■ AUTHOR INFORMATION

Corresponding Authors

*E-mail: gerard.buono@univ-amu.fr.

*E-mail: herve.clavier@univ-amu.fr.

Notes

The authors declare no competing financial interest.

■ ACKNOWLEDGMENTS

This work was supported by the Ministère de l'Enseignement Supérieur et de la Recherche (L.G. Ph.D. grant), the CNRS, AMU, and Centrale Marseille. We gratefully acknowledge Dr. Jean-Valère Naubron, Grégory Excoffier, Dr. Valérie Monnier, and Christophe Chendo (Spectropole, Fédération des Sciences Chimiques de Marseille) for respectively the IR, elemental analyses, and MS analyses as well as Dr. Julie Broggi for useful comments on the manuscript.

■ REFERENCES

- (1) For reviews on the coordination chemistry of phosphinous acids, secondary phosphines, and related compounds, see: (a) Roundhill, D. M.; Sperline, R. P.; Beaulieu, W. B. *Coord. Chem. Rev.* **1978**, *26*, 263–279. (b) Walther, B. *Coord. Chem. Rev.* **1984**, *60*, 67–105. (c) Appleby, T.; Woollins, J. D. *Coord. Chem. Rev.* **2002**, *235*, 121–140.
- (2) Christiansen, A.; Li, C.; Garland, M.; Selent, D.; Ludwig, R.; Spannenberg, A.; Baumann, W.; Franke, R.; Börner, A. *Eur. J. Org. Chem.* **2010**, 2733–2741.
- (3) Martin, D.; Moraleda, D.; Achard, T.; Giordano, L.; Buono, G. *Chem.—Eur. J.* **2011**, *17*, 12729–12740.

(4) Kapoor, P. N.; Saraswati, R.; McMahon, I. J. *Inorg. Chim. Acta* **1985**, *110*, 63–68.

(5) Cotton, F. A.; Kibala, P. A.; Miertschin, C. S. *Inorg. Chem.* **1991**, *30*, 548–553. Teo, S.; Weng, Z.; Hor, T. S. A. *Organometallics* **2008**, *27*, 4188–4192.

(6) (a) Doux, M.; Ricard, L.; Mathey, F.; Le Floch, P.; Mézailles, N. *Eur. J. Inorg. Chem.* **2003**, 687–698. (b) Baker, R. J.; Bettentrup, H.; Jones, C. *Acta Crystallogr. C* **2003**, *59*, m339–m341. (c) Dornhaus, F.; Scholz, S.; Sängler, L.; Bolte, M.; Wagner, M.; Lerner, H. W. *Z. Anorg. Allg. Chem.* **2009**, *635*, 2263–2272.

(7) (a) Pascu, S. I.; Coleman, K. S.; Cowley, A. R.; Green, M. L. H.; Rees, N. H. *New J. Chem.* **2005**, *29*, 385–397. (b) Gushwa, A. F.; Belabassi, Y.; Montchamp, J.-L.; Richards, A. F. J. *Chem. Crystallogr.* **2009**, *39*, 337–347. (c) Gentschow, S.-A.; Kohl, S. W.; Heinemann, F. W.; Wiedemann, D.; Grohmann, A. *Z. Naturforsch.* **2010**, *65b*, 238–250.

(8) Magiera, D.; Szmigielska, A.; Pietrusiewicz, K. M.; Duddeck, H. *Chirality* **2004**, *16*, 57–64.

(9) Li, G. Y. *Angew. Chem., Int. Ed.* **2001**, *40*, 1513–1516.

(10) For reviews on the use of metal-SPO/PA in catalysis, see: (a) Ackermann, L. *Isr. J. Chem.* **2010**, *50*, 652–663. (b) Shaikh, T. M.; Weng, C.-M.; Hong, F.-E. *Coord. Chem. Rev.* **2012**, *256*, 771–803.

(11) Donets, P. A.; Cramer, N. *J. Am. Chem. Soc.* **2013**, *135*, 11772–11775.

(12) Schröder, F.; Tugny, C.; Salanouve, E.; Clavier, H.; Giordano, L.; Moraleda, D.; Gimbert, Y.; Mouries-Mansuy, V.; Goddard, J.-P.; Fensterbank, L. *Organometallics* **2014**, *33*, 4051–4056.

(13) (a) Bigeault, J.; Giordano, L.; Buono, G. *Angew. Chem., Int. Ed.* **2005**, *44*, 4753–4757. (b) Bigeault, J.; De Riggi, I.; Gimbert, Y.; Giordano, L.; Buono, G. *Synlett* **2008**, 1071–1075. (c) Gatineau, D.; Moraleda, D.; Naubron, J.-V.; Bürgi, T.; Giordano, L.; Buono, G. *Tetrahedron: Asymmetry* **2009**, *20*, 1912–1917.

(14) (a) Bigeault, J.; Giordano, L.; De Riggi, I.; Gimbert, Y.; Buono, G. *Org. Lett.* **2007**, *9*, 3567–3570. (b) Achard, T.; Lepionier, A.; Gimbert, Y.; Clavier, H.; Giordano, L.; Tenaglia, A.; Buono, G. *Angew. Chem., Int. Ed.* **2011**, *50*, 3552–3556.

(15) (a) Jiang, X.-B.; Minnaard, A. J.; Hessen, B.; Feringa, B. L.; Duchateau, A. L. L.; Andrien, J. G. O.; Boogers, J. A. F.; de Vries, J. G. *Org. Lett.* **2003**, *5*, 1503–1506. (b) Jiang, X.-B.; van den Berg, M.; Minnaard, A. J.; Feringa, B. L.; de Vries, J. G. *Tetrahedron: Asymmetry* **2004**, *15*, 2223–2229. (c) Landert, H.; Spindler, F.; Wyss, A.; Blaser, H.-U.; Pugin, B.; Ribourduille, Y.; Gschwend, B.; Ramalingam, B.; Pfaltz, A. *Angew. Chem., Int. Ed.* **2010**, *49*, 6873–6876.

(16) (a) Ackermann, L. *Org. Lett.* **2005**, *7*, 3123–3125. (b) Ackermann, L.; Althammer, A.; Born, R. *Angew. Chem., Int. Ed.* **2006**, *45*, 2619–2622. (c) Ackermann, L.; Mulzer, M. *Org. Lett.* **2008**, *10*, 5043–5045. (d) Ackermann, L. *Acc. Chem. Res.* **2014**, *47*, 281–295.

(17) Rafter, E.; Gutmann, T.; Löw, F.; Buntkowsky, G.; Philippot, K.; Chaudret, B.; van Leeuwen, P. W. N. M. *Catal. Sci. Technol.* **2013**, *3*, 595–599.

(18) (a) Oshiki, T.; Muranaka, M. *PCT Int. Appl.*, WO 2012/017966, 2012. (b) Knapp, S. M. M.; Sherbow, T. J.; Yelle, R. B.; Juliette, J. J.; Tyler, D. R. *Organometallics* **2013**, *32*, 3744–3752. (c) Tomás-Mendivil, E.; Suárez, F. L.; Diez, J.; Cadierno, V. *Chem. Commun.* **2014**, *50*, 9661–9664.

(19) (a) Krafczyk, R.; Thönnessen, H.; Jones, P. G.; Schmutzler, R. J. *Fluorine Chem.* **1997**, *83*, 159–166. (b) Chan, E. Y. Y.; Zhang, Q.-F.; Sau, Y.-K.; Lo, S. M. F.; Sung, H. H. Y.; Williams, I. D.; Haynes, R. K.; Leung, W.-H. *Inorg. Chem.* **2004**, *43*, 4921–4926.

(20) den Reijer, C. J.; Würle, M.; Pregosin, P. S. *Organometallics* **2000**, *19*, 309–316.

(21) Robertson, I. W.; Stephenson, T. A. *Inorg. Chim. Acta* **1980**, *45*, L215–L216.

(22) Torres-Lubián, R.; Rosales-Hoz, M. J.; Arif, A. M.; Ernst, R. D.; Paz-Sandoval, M. A. *J. Organomet. Chem.* **1999**, *585*, 68–82.

(23) In our hands, dmsO or cod ligands could not be displaced by secondary phosphine oxides nor phosphinous acids from $\text{Ru}(\text{II})\text{Cl}_2(\text{dmsO})_4$ and $\text{Ru}(\text{II})\text{Cl}_2(\text{cod})$, respectively. Upon thermal activa-

tion, it was possible to replace PPh_3 by a phosphinous acid in the $\text{Ru(II)Cl}_2(\text{PPh}_3)$ complex; however the cooling of the reaction mixture regenerated the initial complex.

- (24) For similar observations, see refs 3, 4, and 7.
- (25) The typical ν_{PO} of free SPO is 1160–1165 cm^{-1} .
- (26) *Like* and *unlike* are used as stereodescriptors for diastereomers with two chirality elements. When the two chirality elements are both *R* or both *S*, the molecular entity is described as having a relationship *like*, when one chirality element is *R* and the other *S*, the molecular entity is described as having a relationship *unlike*. (a) IUPAC Compendium of Chemical Terminology; 2014; p 814. The *like* and *unlike* topicities specify the relationship between the absolute configurations of the reactant enantiomers. (b) Seebach, D.; Prelog, V. *Angew. Chem., Int. Ed. Engl.* **1982**, *21*, 654–660.
- (27) Since we were unable to isolate the side-ruthenium complex accounting for the mass balance, we assumed that degradation occurred.
- (28) Clavier, H.; Nolan, S. P. *Chem. Commun.* **2010**, *46*, 841–861.
- (29) (a) Poater, A.; Cosenza, B.; Correa, A.; Giudice, S.; Ragone, F.; Scarano, V.; Cavallo, L. *Eur. J. Inorg. Chem.* **2009**, 1759–1766. (b) <https://www.molnac.unisa.it/OMtools/sambvca.php>.
- (30) Seddon, E. A.; Seddon, K. R. *The Chemistry of Ruthenium*; Elsevier: Amsterdam, 1984; Chapter 9, pp 341–890.
- (31) Tolman, C. A. *Chem. Rev.* **1977**, *77*, 313–348.
- (32) Chatani, N.; Inoue, H.; Ikeda, T.; Murai, S. *J. Org. Chem.* **2000**, *65*, 4913–4918.
- (33) With the exception of complex **6c**, all complexes **6** are perfectly stable in solution. However, ^{31}P NMR monitoring experiments showed that in the presence of silver salt and the absence of substrate, complexes **6** are poorly stable with a release of PA ligands.
- (34) The mechanistic considerations were based on the mechanism proposed by Murai, ref 32.
- (35) Bour, C.; Monot, J.; Tang, S.; Guillot, R.; Farjon, J.; Gandon, V. *Organometallics* **2014**, *33*, 594–599.
- (36) (a) Hashmi, A. S.K. In *Silver in Organic Chemistry*; Harmata, M., Ed.; Wiley: Hoboken, 2010; pp 357–379. (b) Weibel, J.-M.; Blanc, A.; Pale, P. *Chem. Rev.* **2008**, *108*, 3149–3173.
- (37) Achard, T.; Giordano, L.; Tenaglia, A.; Gimbert, Y.; Buono, G. *Organometallics* **2010**, *29*, 3936–3950 and references therein.